Antiviral activity of influenza A virus defective interfering particles against SARS-CoV-2 replication *in vitro* through stimulation of innate immunity

Rand U.[1,*], Kupke S.Y.[2,*,#], Shkarlet H.[3,4,*], Hein M.D.[5], Hirsch T.[3], Marichal-Gallardo P.[2], Cicin-Sain L.[1,6,7], Reichl U.[2,5], Bruder D.[3,4]

[1]Department of Vaccinology and Applied Microbiology, Helmholtz Centre for Infection Research, Braunschweig, Germany

[2]Bioprocess Engineering, Max Planck Institute for Dynamics of Complex Technical Systems, Magdeburg, Germany

[3]Immune Regulation Group, Helmholtz Centre for Infection Research, Braunschweig, Germany

[4]Institute of Medical Microbiology, Infection Prevention and Control, Infection Immunology Group, Health Campus Immunology, Infectiology and Inflammation, Otto von Guericke University Magdeburg, Magdeburg, Germany

[5]Bioprocess Engineering, Otto von Guericke University Magdeburg, Magdeburg, Germany

[6]German Centre for Infection Research, Hannover-Braunschweig Site, Braunschweig, Germany

[7]Centre for Individualized Infection Medicine, a joint venture of Helmholtz Centre for Infection Research and Medical School Hannover, Germany

[*]First author

[#]Correspondence: kupke@mpi-magdeburg.mpg.de

Abstract

SARS-CoV-2 causing COVID-19 emerged in late 2019 and resulted in a devastating pandemic. Although the first approved vaccines were already administered by the end of 2020, worldwide vaccine availability is still limited. Moreover, immune escape variants of the virus are emerging against which the current vaccines may confer only limited protection. Further, existing antivirals and treatment options against COVID-19 only show limited efficacy. Influenza A virus (IAV) defective interfering particles (DIPs) were previously proposed not only for antiviral treatment of the influenza disease but also for pan-specific treatment of interferon (IFN)-sensitive respiratory virus infections. To investigate the applicability of IAV DIPs as an antiviral for the treatment of COVID-19, we conducted *in vitro* co-infection experiments with cell culture-derived DIPs and the IFN-sensitive SARS-CoV-2 in human lung cells. We show that treatment with IAV DIPs leads to complete abrogation of SARS-CoV-2 replication. Moreover, this inhibitory effect was dependent on janus kinase/signal transducers and activators of transcription (JAK/STAT) signaling. Further, our results suggest boosting of IFN-induced antiviral activity by IAV DIPs as a major contributor in suppressing SARS-CoV-2 replication. Thus, we propose IAV DIPs as an effective antiviral agent for treatment of COVID-19, and potentially also for suppressing the replication of new variants of SARS-CoV-2.

Keywords: SARS-CoV-2, COVID-19, antiviral, influenza A virus, defective interfering particles, OP7, DI244, innate immunity

46 # Introduction

47 Severe acute respiratory syndrome coronavirus 2 (SARS-CoV-2), causing coronavirus
48 disease 2019 (COVID-19), poses a severe burden to public health, economy and
49 society. To date, almost four million deaths were reported in the context of SARS-
50 CoV-2 infection (WHO, covid19.who.int). Starting early 2020, there has been a
51 unprecedented race for the development of novel vaccines, their production, and
52 execution of safety and immunogenicity studies in clinical trials (Krammer, 2020,
53 Walsh et al., 2020, Voysey et al., 2020, Jackson et al., 2020, Logunov et al., 2020,
54 Palacios et al., 2020). These efforts led to the vaccination of the first individuals
55 outside clinical trials in late 2020. While vaccination typically provides the best
56 protection against virus infections and disease onset, the worldwide manufacturing
57 capacity of COVID-19 vaccines, and the infrastructure required for vaccination are
58 still limited. In addition, vaccination is a prophylactic measure and not applicable for
59 therapeutic treatment of acute infections. Therefore, as an alternative option, the
60 development of antivirals for treatment of COVID-19 is essential. Yet, remdesivir (in
61 clinical use) showed only limited efficacy (Wang et al., 2020, Beigel et al., 2020, Pan
62 et al., 2020), while other repurposed drug candidates (e.g., hydroxychloroquine and
63 lopinavir-ritonavir) showed a lack of efficacy (Boulware et al., 2020, Cao et al.,
64 2020). In addition, corticosteroids (i.e., dexamethasone (Tomazini et al., 2020)) and
65 cocktails of monoclonal antibodies (e.g., bamlanivimab (Chen et al., 2020b)) are
66 used in the clinic and show an antiviral effect. However, the appearance of new
67 SARS-CoV-2 variants poses a constant risk to lose efficacy of highly specific
68 treatments, including vaccination and therapeutic antibodies. Thus, there is a need to

69 develop more broadly acting, cost-effective antivirals that ideally are easily scalable
70 in production.

71 Influenza A virus (IAV) defective interfering particles (DIPs) were previously
72 proposed for antiviral treatment against IAV infections (Zhao et al., 2018, Vignuzzi
73 and Lopez, 2019, Meir et al., 2020, Tapia et al., 2019, Yang et al., 2019, Harding et
74 al., 2019, Tanner et al., 2016, Huo et al., 2020b, Kupke et al., 2020), but also for
75 pan-specific treatment of other respiratory viral diseases (Dimmock and Easton,
76 2014, Dimmock and Easton, 2015). IAV DIPs typically carry a large internal deletion
77 in their genome, rendering them defective in virus replication (Alnaji and Brooke,
78 2020, Ziegler and Botten, 2020, Andreu-Moreno and Sanjuan, 2020). Furthermore,
79 DIPs suppress and interfere specifically with homologous viral replication in a co-
80 infection scenario, a process known as replication interference. As a result,
81 administration of IAV DIPs to mice resulted in full protection against an otherwise
82 lethal IAV infection (Dimmock et al., 2008, Huo et al., 2020b, Hein et al., 2021c, Hein
83 et al., 2021a). In the ferret model, treatment of IAV-infected animals resulted in a
84 reduced severity of disease pathogenesis (Dimmock et al., 2012). Intriguingly, mice
85 were also protected against a lethal infection with the unrelated influenza B virus
86 (Scott et al., 2011) and pneumonia virus of mice (PVM) from the family
87 *Paramyxoviridae* (Easton et al., 2011). Here, protection was not attributed to
88 replication interference but to the ability of IAV DIPs to stimulate innate immunity.

89 SARS-CoV-2 replication seems to modulate and inhibit the interferon (IFN) response
90 in infected target cells (Chen et al., 2020a, Konno et al., 2020, Lei et al., 2020). Still,
91 it was also shown to be susceptible to inhibition by exogenously added IFNs *in vitro*
92 (Busnadiego et al., 2020, Felgenhauer et al., 2020), *in vivo* (Hoagland et al., 2021)

93 and in clinical trials (Monk et al., 2020). Therapies using recombinant IFNs, however,
94 are cost intensive and pose the risk of unwanted side effects including the formation
95 of auto-antibodies against the cytokine (reviewed in (Sleijfer et al., 2005)). To
96 prevent this, we wondered whether IAV DIPs would be able to suppress SARS-CoV-2
97 replication through their ability to stimulate a physiological IFN response in target
98 cells. To test this, we produced two promising candidate DIPs, a prototypic, well-
99 characterized conventional IAV DIP "DI244" (Dimmock and Easton, 2014), and a
100 novel type of IAV DIP "OP7", that contains point mutations instead of a large internal
101 deletion in the genome (Kupke et al., 2019), using a cell culture-based production
102 process (Hein et al., 2021c, Hein et al., 2021a, Hein et al., 2021b).

103 Here, we used Calu-3 cells (human lung cancer cell line) for *in vitro* co-infection
104 experiments with SARS-CoV-2 and DI244 or OP7, respectively. Both DIPs were able
105 to completely inhibit SARS-CoV-2 replication and spreading in a range comparable to
106 IFN-β or remdesivir treatment. Moreover, we show that the inhibitory effect of IAV
107 DIPs was due to their ability to induce innate immune responses that signal via janus
108 kinase/signal transducers and activators of transcription (JAK/STAT). In addition, our
109 results show that IAV DIP infection triggers elevated host cell type-I and type-III IFN
110 production and subsequent IFN-induced antiviral activity. Thus, we propose IAV DIPs
111 as effective antiviral agents for the treatment of COVID-19 and, potentially as
112 universal antiviral agents not only against different influenza subtypes but also
113 against other (including newly emerging) IFN-sensitive respiratory viruses.

114 # Results

115 ## SARS-CoV-2 replication is abrogated by IAV DIP treatment *in vitro*

116 In order to test the antiviral efficacy of IAV DIPs on replication of SARS-CoV-2, we
117 conducted *in vitro* co-infection experiments in Calu-3 cells. For this, we infected cells
118 with SARS-CoV-2 (multiplicity of infection (MOI) = 0.03) and highly concentrated IAV
119 DIPs (DI244 or OP7), respectively, from cell culture-based production and
120 membrane-based chromatographic purification (Marichal-Gallardo et al., 2017, Hein
121 et al., 2021c, Hein et al., 2021a). At 3 days post infection (dpi), cells were stained for
122 the SARS-CoV-2 spike (S) protein (Fig. 1A). Indeed, S protein expression was
123 significantly reduced in cells co-treated with DI244 or OP7 compared to cells infected
124 with SARS-CoV-2 only, indicating suppression of SARS-CoV-2 replication by IAV DIP
125 co-infection. In agreement with this observation, images from live-cell microscopy
126 show a clearly reduced cytopathic effect upon DIP co-infection from ~36 hpi on (Fig.
127 1B).

128 In order to test the antiviral efficiency of IAV DIPs in comparison with clinically
129 relevant antivirals, dose-effect curves were generated by testing different
130 concentrations of IAV DIPs for the treatment of SARS-CoV-2-infected cells (Fig. 1C).
131 As a read-out for SARS-CoV-2 replication, we determined the infectious titer from
132 supernatants at 3 dpi using plaque assays with Vero-6 cells. Please note that
133 infection with only defective, replication-incompetent IAV DIPs does not result in the
134 release of progeny virions, as demonstrated by negative plaque titers (Hein et al.,
135 2021c, Hein et al., 2021a). Strikingly, SARS-CoV-2 replication was severely
136 diminished upon IAV DIP co-infection. In particular, at high DI244 and OP7

concentrations, no SARS-CoV-2 plaque titers were detectable anymore, while untreated cells showed a titer of 7.5 x 10^4 plaque-forming units (pfu)/mL. Suppression of SARS-CoV-2 replication decreased with increasing dilution of DIPs. Remarkably, though, the treatment with both DIPs at a dilution of 1:1000 still resulted in a pronounced inhibition of SARS-CoV-2 replication, corresponding to a 26-fold and 210-fold reduction in plaque titers for DI244 and OP7 treatment, respectively. For comparison, we also tested the inhibitory capacity of IFN-β or remdesivir treatment on SARS-CoV-2 replication in infected target cells. Both agents were also able to diminish SARS-CoV-2 plaque titers to below the limit of detection (LOD), until a concentration of 633 U/mL for IFN-β and 0.32 μM for remdesivir. Yet, inhibiting effects ceased significantly faster with increasing dilutions, most apparently observed for remdesivir, for which treatment with a concentration of 0.03 μM (1:10 dilution) already did not result an inhibitory effect anymore.

Fig. 1D illustrates residual SARS-CoV-2 inhibition caused by inactivated DIPs. These DIPs were previously UV-irradiated until no interfering efficacy against IAV replication was observed anymore *in vitro* (Hein et al., 2021c, Hein et al., 2021a), indicating the degradation of the causative interfering agent, i.e., the genomic defective interfering (DI) viral RNA (vRNA). The finding that inhibition caused by active DIPs was more efficient suggests a specific interfering activity of active IAV DIPs with SARS-CoV-2 replication. Of note, active DIPs still conferred a pronounced antiviral effect even when applied 24 h after preceding SARS-CoV-2 infection (Fig. 1E).

In conclusion, treatment with both DI244 and OP7 IAV DIPs completely abolished SARS-CoV-2 replication during *in vitro* co-infections. While the inhibitory potential

160 was comparable to IFN-β and remdesivir treatment, the antiviral effects of IAV DIPs

161 were more sustained with increasing dilution.

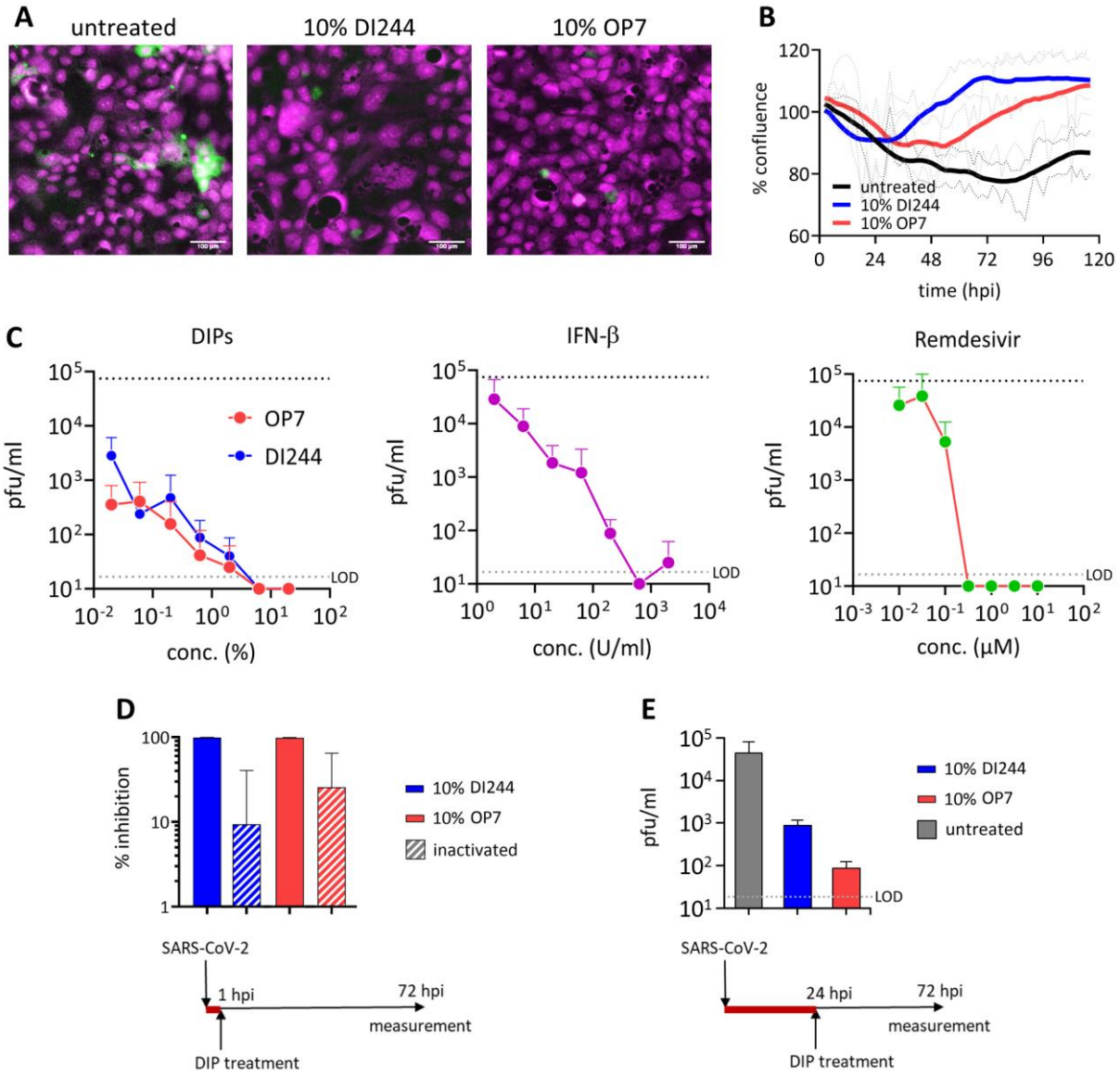

Fig. 1. Inhibition of SARS-CoV-2 replication and spreading by IAV DIPs. SARS-CoV-2-infected Calu-3 cells (MOI=0.03) were treated with IAV DIPs (DI244 or OP7), IFN-β, or remdesivir at 1 hour post infection (hpi). For DI244 and OP7 treatment, chromatographically purified and highly concentrated cell culture-derived DIP material (Hein et al., 2021c, Hein et al., 2021a) was used. % (v/v) indicates the fraction with respect to the cell culture volume of 100 µL. Stock concentration, 5.6 × 10^8 and 1.12 × 10^{11} DI vRNAs/mL for DI244 and OP7, respectively. (**A**) Immunofluorescence analysis of the SARS-CoV-2 S protein expression (green, magenta: DNA) at 3 dpi. Scale bar, 100 µm. (**B**) Cytopathic effect. Confluence (% of initial) was measured by live-cell microscopy at 2 h intervals. Thick lines represent smoothened data (Savitzky-Golay filter), dotted lines show SD of original data (n=2, independent experiments). (**C**) Effective concentration range of DI244 and OP7 compared to IFN-β and remdesivir. Viral titers were determined from the supernatant at 3 dpi by plaque assay. Upper dotted line indicates virus titer in untreated cells, lower dotted line shows the LOD. Independent experiments were conducted; mean ± SD (n=3) is shown. (**D**) SARS-CoV-2 growth inhibition by active and inactive DIPs. SARS-CoV-2 infected cells were treated with active or UV-

177 inactivated DIPs at 1 hpi. Percentage inhibition of viral growth relative to mock treatment is shown;
178 mean ± SEM (n=4) is depicted. (**E**) DIP superinfection 24 h post SARS-CoV-2 infection. Independent
179 experiments were conducted; mean ± SD (n=2) is shown.

180 **IAV DIP infection enhances type-I and type-III IFN responses and inhibit**
181 **SARS-CoV-2 replication via Janus-kinase signaling**

182 Next, to investigate our hypothesis whether inhibition of SARS-CoV-2 replication by
183 DIPs was due to their ability to stimulate the IFN system, we used ruxolitinib in co-
184 infection experiments. This small molecule drug is an efficient inhibitor of JAK, which
185 are key effectors in the IFN system. Upon IFN sensing, JAKs typically recruit STATs,
186 ultimately leading to the upregulation of IFN-stimulated gene (ISGs). ISGs encode for
187 effector molecules that limit viral replication by inducing an antiviral state in the
188 infected as well as uninfected neighboring cells. Fig. 2 shows the results of SARS-
189 CoV-2 and IAV DIP co-infection upon treatment with ruxolitinib. While DI244 and
190 OP7 co-infection almost completely inhibited SARS-CoV-2 replication, additional
191 treatment with ruxolitinib abrogated the suppressive effect of both IAV DIPs.
192 Specifically, virus titers under JAK signaling inhibition were comparable to SARS-CoV-
193 2 infection in the absence of DIPs. These results suggest a major contribution of
194 unspecific innate immune activation by IAV DIPs in interfering with SARS-CoV-2
195 replication.

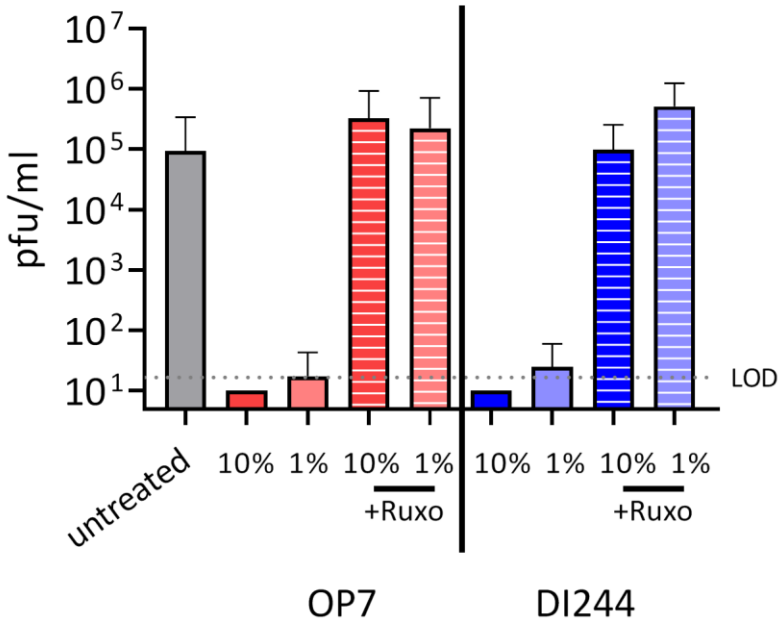

196

197 **Fig. 2. Suppression of SARS-CoV-2 replication by IAV DIPs under JAK inhibition.** SARS-CoV-
198 2-infected Calu-3 cells (MOI=0.03) were co-infected with IAV DIPs (DI244 or OP7) at 1 hpi in the
199 presence of absence of ruxolitinib (JAK inhibitor). % (v/v) indicates the fraction of DIPs (highly
200 concentrated cell culture-derived material (Hein et al., 2021c, Hein et al., 2021a) with respect to the
201 cell culture volume of 100 µL. Viral titers were determined from the supernatant at 3 dpi by plaque
202 assay. Dotted line shows the LOD. Independent experiments were conducted; mean ± SD (n=4) is
203 depicted.

204 In order to shed light onto correlates of IAV DIP-mediated SARS-CoV-2 suppression,
205 we used real-time RT-qPCR for quantification of gene expression to assess innate
206 immune responses during co-infections in more detail (Fig. 3A). We observed a
207 significant upregulation of type I and III IFN (i.e., *IFNB1* and *IFNL1*, respectively)
208 expression at early times following IAV DIP and SARS-CoV-2 co-infection compared
209 to SARS-CoV-2 single infection. Specifically, we detected one to two $\log_{10}$ higher
210 *IFNB1* and *IFNL1* mRNA levels at 6 hpi. In addition, canonical antiviral gene
211 expression, indicated by *MX1* and *RSAD2,* was elevated. This early upregulation of
212 innate immune responses may well explain the strong antiviral activity of DI244 and
213 OP7 against SARS-CoV-2 replication. In agreement with this, we detected significant
214 uptake of the non-replicating DI244 and OP7 vRNA (~10E3 molecules/cell) (Fig. 4A)
215 and concomitant upregulation of *DDX58* (Fig. 4B), encoding for retinoic acid inducible
216 gene I (RIG-I); a pattern recognition receptor (PRR) critical for detection of viral
217 nucleic acids and initiation of cellular antiviral responses. The significantly lower
218 levels of DI vRNAs detected for cells treated with inactive DIPs can be explained by
219 their efficient degradation by the inactivation procedure (i.e., UV-irradiation).
220 As a control, we infected cells with only active or inactive IAV DIPs. Here, only active
221 DIPs were able to mount an elevated innate immune response (Fig. 3A, lower
222 panels). Interestingly, canonical antiviral gene expression (*MX1* and *RSAD2*) was
223 enhanced until 72 hpi for the active DIP-only treatment, implying that DI244 and
224 OP7 can potentially raise a long-lived antiviral ISG response.
225 In line with the results from real-time RT-qPCR, protein levels of secreted IFN-β and
226 IFN-λ3 (investigated using ELISA) were elevated at later times post infection for cells
227 co-infected with IAV DIPs and SARS-CoV-2 compared to cells infected with only

228 SARS-CoV-2 (Fig. 3B and 3C). In conclusion, our results suggest the early stimulation
229 and subsequent boosting of the type-I and type-III IFN response as causative for the
230 inhibiting potential of IAV DIPs against SARS-CoV-2 replication.

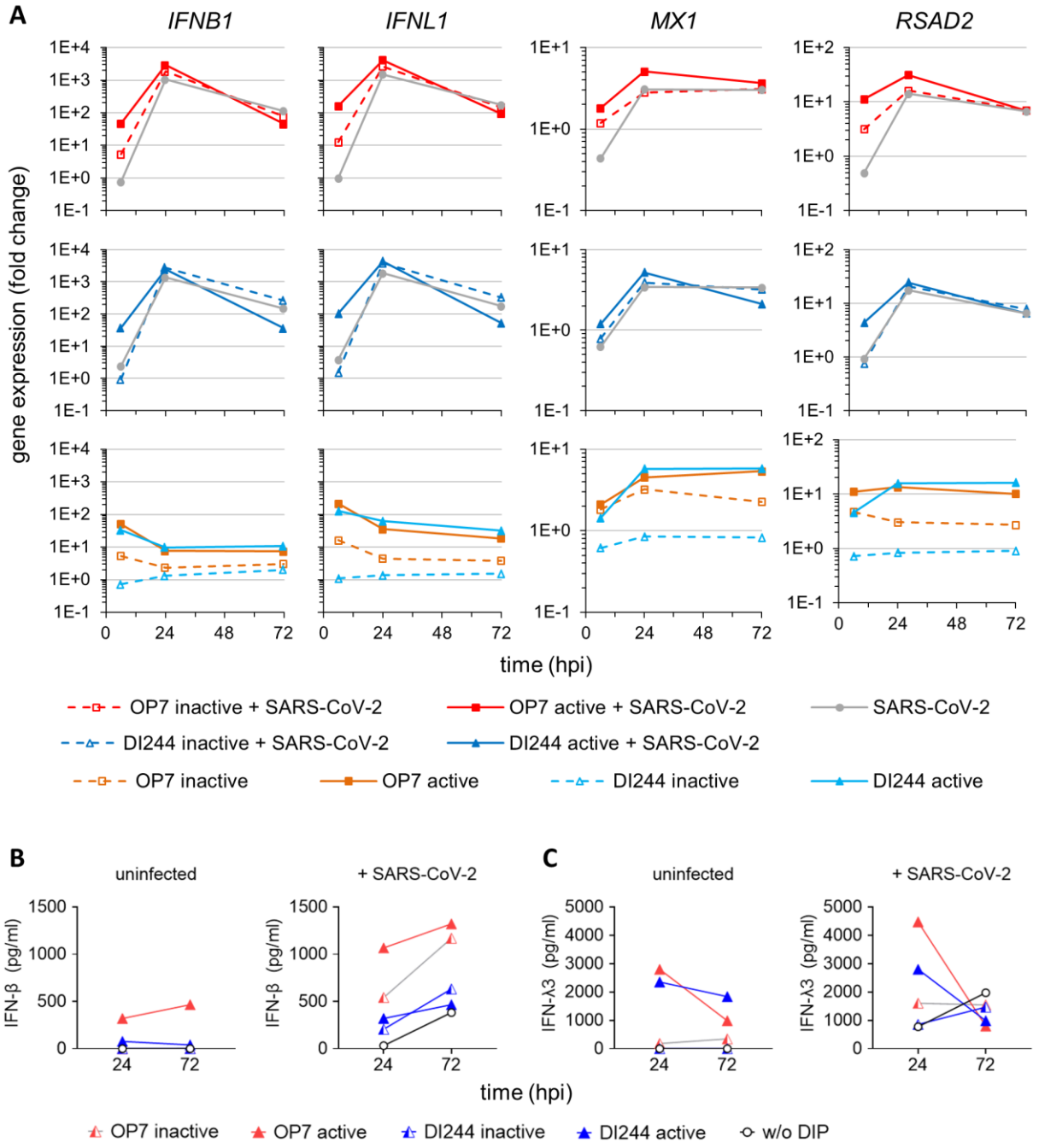

Fig. 3. Stimulation of IFN-induced antiviral activity by IAV DIP infection. SARS-CoV-2-infected Calu-3 cells (MOI=0.03) were treated with IAV DIPs (DI244 or OP7) at 1 hpi. For DI244 and OP7 infection, 10% (v/v) (100 µL culture volume) of highly concentrated cell culture-derived DIP material was used (Hein et al., 2021c, Hein et al., 2021a). At indicated times post infection, infected cells were lysed to allow for total RNA extraction, required for (**A**) gene expression analysis. In addition, supernatants were sampled for (**B** and **C**) quantification of secreted IFNs. Illustration includes data from one experiment. (**A**) Gene expression analysis of SARS-CoV-2 and IAV DIP co-infection. Transcript levels were quantified by real-time RT-qPCR and expressed as fold change (relative to untreated, uninfected cells). (**B** and **C**) Host cell IFN production. Protein levels of IFN-β (**B**) and IFN-λ3 (**C**) were assessed using ELISA.

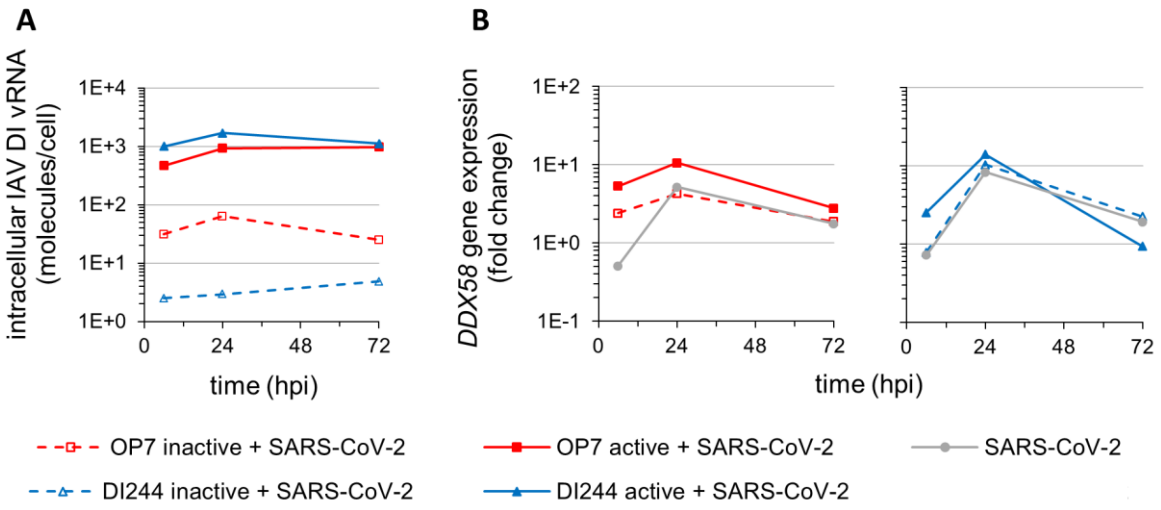

Fig. 4. Cellular uptake of IAV DI vRNAs and *DDX58* expression. SARS-CoV-2-infected Calu-3 cells (MOI=0.03) were treated with IAV DIPs (DI244 or OP7) at 1 hpi. For DI244 and OP7 infection, 10% (v/v) (100 µL culture volume) of highly concentrated cell culture-derived DIP material was used (Hein et al., 2021c, Hein et al., 2021a). At indicated times post infection, cells were lysed to allow for total RNA extraction, required for (**A**) quantification of intracellular DI vRNAs and (**B**) analysis of *DDX58* gene expression. Illustration includes data from one experiment. (**A**) Intracellular DI vRNA levels during SARS-CoV-2 and IAV DIP co-infection. Cells were assayed for viral RNAs by real-time RT-qPCR. (**B**) *DDX58* gene expression analysis. *DDX58* (encoding for RIG-I) transcript levels were quantified by real-time RT-qPCR and expressed as fold change (relative to untreated, uninfected cells).

253 ## Discussion

254 Despite the recent availability of vaccines against COVID-19, options for antiviral
255 treatment are urgently needed for therapeutic application. Here, we show that cell
256 culture-derived IAV DIPs are highly potent inhibitors of SARS-CoV-2 replication in
257 human lung cells. In addition, our data obtained in *in vitro* experiments suggest that
258 suppression of SARS-CoV-2 replication by IAV DIPs is predominantly attributed to
259 their ability to stimulate innate immune responses ultimately inducing an antiviral
260 state in target cells.

261 In the clinic, already approved antivirals for treatment of COVID-19 showed only very
262 limited efficacy. For instance, treatment with the polymerase inhibitor remdesivir did
263 not result in an overall decrease in mortality (Beigel et al., 2020, Pan et al., 2020).
264 For patients receiving supplemental oxygen, however, an improvement in the
265 survival rate from about 4% to 12% was observed (Beigel et al., 2020). In addition,
266 the time required to recover from COVID-19 was decreased by five days (Wang et
267 al., 2020, Beigel et al., 2020). Another option to treat COVID-19 is the use of
268 monoclonal antibodies that target the receptor binding domain of the SARS-CoV-2 S
269 protein, thereby inhibiting engagement with the host cell entry receptor angiotensin-
270 converting enzyme 2 (ACE2) (Hoffmann et al., 2020, Abraham, 2020). Here, it was
271 suggested to use antibody cocktails to prevent the emergence of viral escape
272 variants in treated individuals (Baum et al., 2020). In clinical trials, treatment of
273 outpatients with one such an antibody cocktail (i.e., bamlanivimab) accelerated the
274 decrease in viral load and reduced the fraction of patients requiring hospitalization
275 from 6.3% to 1.6% (Chen et al., 2020b). The administration of the corticosteroid
276 dexamethasone (in clinical use) resulted in an overall lower mortality in critically ill

277 COVID-19 patients (Horby et al., 2020, Sterne et al., 2020). This has a caveat,
278 though, as a decrease in mortality was observed for patients requiring oxygen
279 (including mechanical ventilation), but an increase in mortality was reported for
280 patients not requiring oxygen (Horby et al., 2020). This comparatively little progress
281 in COVID-19 therapy has sparked calls to invest more research into broadly acting
282 antiviral agents against SARS-CoV-2 to combat future pandemics (Dolgin, 2021).

283 Treatment of COVID-19 patients with IFNs has not been approved yet. In general,
284 SARS-CoV-2 infection can modulate and inhibit the IFN response (Chen et al., 2020a,
285 Konno et al., 2020, Lei et al., 2020). In addition, it was recently shown that the host
286 cell entry receptor ACE2 is indeed an ISG, and it was speculated that SARS-CoV-2
287 may exploit the IFN-driven upregulation of ACE2 to enhance infection (Ziegler et al.,
288 2020). However, SARS-CoV-2 replication is, in general, also susceptible to inhibition
289 by exogenously added IFN. For instance, all IFNs (type I, II and III) exhibited potent
290 antiviral activity with SARS-CoV-2 replication *in vitro* (Busnadiego et al., 2020,
291 Felgenhauer et al., 2020), suggesting that the antiviral activities of IFNs can
292 counterbalance any proviral effects derived from ACE2 induction. Yet, note that type-
293 I IFN treatment seems to play an ambiguous role in COVID-19, depending on the
294 stage of the disease (reviewed in (Lee and Shin, 2020)), and also type-III IFNs can
295 contribute to COVID-19 pathogenesis (Broggi et al., 2020). Therefore, therapeutic
296 administration of IFNs (or IAV DIPs) in the future will have to be carefully evaluated
297 with respect to timing. Nevertheless, it was shown that intranasal IFN-I
298 administration (in hamsters) pre- or post-virus challenge can reduce SARS-CoV-2
299 disease burden (Hoagland et al., 2021). Moreover, in a placebo-controlled phase 2
300 clinical trial, administration of inhaled, nebulized IFN-β (to patients already admitted

301 to hospital due to COVID-19 symptoms) resulted in a higher chance of disease
302 improvement and a more rapid recovery from COVID-19 (Monk et al., 2020).

303 In our cell culture experiments, IAV DIPs completely abrogated SARS-CoV-2
304 replication. Notably, the UV-irradiated and thus inactive DIP material (containing
305 degraded DI vRNAs) also showed a residual inhibitory effect. Yet, the observation of
306 a much stronger antiviral effect upon treatment with active DIPs hints to an
307 immunostimulatory activity of active IAV DIPs in the context of SARS-CoV-2
308 suppression. In principle, DIPs are defective in virus replication; therefore, they fail
309 to complete the entire infection cycle. Thus, the genomic DI vRNAs entering the cell
310 cannot multiply, but are typically very well detected by RIG-I (Baum and Garcia-
311 Sastre, 2011), which subsequently leads to the activation of an IFN-response
312 (Rehwinkel et al., 2010), in line with our results. In conclusion, it appears that
313 physically (or chemically) inactivated viral particles are not sufficient to induce a
314 strong antiviral immunity, in contrast to "live" but propagation-incompetent IAV DIPs.
315 With respect to the safety of IAV DIPs for potential clinical application, it is important
316 to note that administration of active DIPs did not cause apparent toxic effects in mice
317 and ferrets (Hein et al., 2021a, Hein et al., 2021c, Dimmock et al., 2008, Dimmock et
318 al., 2012).

319 Our results support the notion that IAV DIPs do not only protect host cells from IAV
320 infection but, in addition, may generally confer protection against other heterologous
321 IFN-sensitive respiratory viruses (Easton et al., 2011, Scott et al., 2011, Dimmock
322 and Easton, 2015). Considering the emergence of new SARS-CoV-2 variants, against
323 which a decreasing efficacy of various vaccines is becoming evident, the unspecific
324 stimulation of innate immunity by IAV DIPs is considered advantageous; in particular,

325 regarding a potential universal efficacy against such new (and future) variants.
326 Furthermore, previous *in vitro* and *in vivo* experiments also revealed an antiviral
327 effect of IAV DIPs against a variety of different IAV subtypes, including pandemic
328 and highly pathogenic avian IAV strains (Dimmock et al., 2008, Dimmock et al.,
329 2012, Zhao et al., 2018, Huo et al., 2020a).

330 Future work to clarify the therapeutic effects of IAV DIPs on the outcome of SARS-
331 CoV-2 infection and to decipher in more detail the underlying mode of action should
332 comprise animal trials in Syrian hamsters or genetically modified humanized K18-
333 hACE2 mice, which are susceptible to SARS-CoV-2 infection and develop a similar
334 respiratory disease compared to human COVID-19 (Kaptein et al., 2020, Boudewijns
335 et al., 2020, Chan et al., 2020, Yinda et al., 2021). Animal experiments will help to
336 elaborate on the potential applicability of IAV DIPs (e.g., administration via a droplet
337 spray) as a pre- and post-exposure treatment for instance in acute SARS-CoV-2
338 outbreak scenarios in the clinics or geriatric institutions. In addition to vaccination,
339 this would represent an interesting option for prophylactic treatment to boost
340 antiviral immunity in persons at acute risk for an infection or for therapeutic
341 treatment during an early phase post infection and as such may prevent fatal COVID-
342 19 outcomes.

343 # Materials and methods

344 ## Cells and viruses

345 Vero-6 cells (ATCC CRL-1586) were maintained in DMEM medium (Gibco, 4.5 g/L
346 glucose, w/o pyruvate) supplemented with 10% fetal calf serum (FCS, Biowest,
347 S1810-6500), 100 IU/mL penicillin, 100 µg/mL streptomycin, 1× GlutaMax (Gibco)
348 and 1× sodium pyruvate (Gibco). Calu-3 cells (ATCC HTB-55) were cultured in MEM
349 (Sigma) supplemented with 10% FCS (Biowest, S1810-6500), 100 IU/mL penicillin,
350 100 µg/mL streptomycin, 1× GlutaMax (Gibco) and 1× sodium pyruvate (Gibco).
351 Caco-2 cells (ATCC HTB-37) were grown in MEM (Gibco) supplemented with 20%
352 FCS (Biowest, S1810-6500), 100 IU/mL penicillin, 100 µg/mL streptomycin, 1×
353 GlutaMax (Gibco) and 1× non-essential amino acid solution (Gibco). All cells were
354 maintained or infected at 37°C in a 5% CO_2 atmosphere.

355 The IAV DIPs DI244 and OP7 were produced in a cell culture-based process using a
356 500 mL laboratory scale stirred tank bioreactor, followed by purification and
357 concentration by membrane-based steric exclusion chromatography (Marichal-
358 Gallardo et al., 2017, Marichal-Gallardo et al., 2021), as described previously (Hein et
359 al., 2021c, Hein et al., 2021a). Production titers of 3.3 and 3.67 log hemagglutination
360 (HA) units/100µL (quantified by the HA assay (Kalbfuss et al., 2008)) and 5.6×10^8
361 and 1.12×10^{11} DI vRNAs/mL (quantified by real-time RT-qPCR (Kupke et al., 2019,
362 Hein et al., 2021c, Wasik et al., 2018)) were achieved for DI244 and OP7,
363 respectively.

364 The SARS-CoV-2 isolate hCoV-19/Croatia/ZG-297-20/2020 was used. All experiments
365 with infectious SARS-CoV-2 were performed in the BSL-3 facility at the Helmholtz

366 Centre for Infection Research (Braunschweig, Germany). The SARS-CoV-2 seed virus
367 was produced in Caco-2 cells, and virus particles were enriched in Vivaspin 20
368 columns (Sartorius Stedim, Biotech) via centrifugation. Collected virus was stored at -
369 80°C. SARS-CoV-2 titers were quantified by plaque assay.

370

371 **SARS-CoV-2 quantification**

372 Quantification of SARS-CoV-2 was performed by plaque assay. Samples were serially
373 diluted in 10-fold steps, and used to infect a confluent monolayer of Vero-6 cells (on
374 96-well plates) for 1 h. Then, the inoculum was removed and cells were overlaid with
375 cell culture medium containing 1.5% methyl-cellulose (SIGMA, #C9481-500). At 3
376 dpi, cells were fixed with 6% formaldehyde and stained with crystal violet. Wells
377 were imaged using a Sartorius IncuCyte S3 (4× objective, whole-well scan) and
378 plaque counts were determined.

379

380 **SARS-CoV-2 infection and antiviral treatment**

381 Confluent Calu-3 cells in 96-well plates (~6×10^4 cells/well) were infected with
382 SARS-CoV-2 (2000 PFU per well). At 1 or 24 hpi, we added active or inactive IAV
383 DIPs (DI244 or OP7) at indicated fractions (% v/v) with respect to the cell culture
384 volume of 100 µL. Whenever indicated, we additionally added 0.8 µM ruxolitinib
385 (Cayman Chemical, Cat. #Cay11609-1) to these wells. Alternatively, remdesivir
386 (MedChem Express, #HY-104077) or human IFN-β-1A (PBL assay science, #11415-
387 1) (instead of IAV DIPs) were added at indicated concentrations at 1 hpi.

388 Supernatants were collected at indicated time points for quantification of SARS-CoV-2
389 titers (plaque assay) and for protein quantification of secreted IFNs using
390 commercially available ELISA kits (see below). In addition, infected cells were lysed
391 using solution "RL" for subsequent total RNA extraction using the "innuPREP RNA
392 Mini Kit 2.0" (Analytik Jena, #845-KS-2040050), according to the manufacturer's
393 instructions, for gene expression analysis via real-time RT-qPCR.

394

395 **Immunofluorescence staining**

396 (Co-)infected cells were fixed with 6% paraformaldehyde in PBS for 1 h at room
397 temperature, followed by washing with PBS. Cells were permeabilized with 0.1%
398 Triton X-100 in PBS for 10 min at room temperature, washed with PBS, and blocked
399 with 2% BSA in PBS for 1 h. Antibody labelling was performed with mouse anti-
400 SARS-CoV-2 S protein (Abcalis, clone AB68-A09, #ABK68-A09-M) and secondary
401 antibody anti-mouse Alexa488 (Cell Signaling Technology, #4408), each step
402 followed by three washing steps with PBS containing 0.05% Tween-20. Finally, cells
403 were overlaid with Vectashield mouting medium (Biozol, #VEC-H-1000).

404

405 **Assessment of IFN production by host cells**

406 Supernatants of (co-)infected cells were assessed for IFN-β and IFN-λ3 levels using
407 corresponding "Quantikine" ELISA kits (R&D Systems, #DIFNB0 and #D28B00,
408 respectively) according to the manufacturer's instructions.

409

410 **Gene expression analysis**

411 mRNA expression levels in (co-)infected cells were assessed using real-time RT-
412 qPCR. 500 ng of total RNA was reverse transcribed using an oligo(dT) primer and the
413 enzyme "Maxima H Minus" (both from Thermo Scientific) according to the
414 manufacturer's instructions. Next, qPCR was conducted using the "Rotor-Gene Q"
415 real-time PCR cycler (Qiagen) and the following primers: *IFNB1*, 5'-
416 CATTACCTGAAGGCCAAGGA-3' and 5'-CAGCATCTGCTGGTTGAAGA-3'; *IFNL1*, 5'-
417 GGTGACTTTGGTGCTAGGCT-3' and 5'-TGAGTGACTCTTCCAAGGCG-3'; *MX1*, 5'-
418 GTATCACAGAGCTGTTCTCCTG-3' and 5'-CTCCCACTCCCTGAAATCTG-3'; *RSAD2*, 5'-
419 CCCCAACCAGCGTCAACTAT-3' and 5'-TGATCTTCTCCATACCAGCTTCC-3'; *GAPDH*, 5'-
420 CTGGCGTCTTCACCACCATGG-3' and 5'-CATCACGCCACAGTTTCCCGG-3' (all
421 sequences from (Busnadiego et al., 2020)); *DDX58*, 5'-TGCAAGCTGTGTGCTTCTCT-3'
422 and 5'-TCCTGAAAAACTTCTGGGGCT-3' (Zhang et al., 2008). The qPCR reaction
423 mixture (10 µL) comprised 1× Rotor-Gene SYBR green PCR mix (Qiagen), 500 nM of
424 each primer, and 4 µL of cDNA. DNA denaturation was conducted for 5 min at 95°C,
425 followed by 40 PCR cycles: 10 s at 95°C and 20 s at 62°C. Gene expression was
426 calculated using the ΔΔCT method using *GAPDH* as the reference gene and
427 expressed as fold change relative to untreated, uninfected cells.

428

429 **Quantification of intracellular IAV DI vRNAs**

430 Real-time RT-qPCR was used for quantification of intracellular DI vRNAs from purified
431 total RNA, as described previously (Hein et al., 2021a, Hein et al., 2021c, Kupke et
432 al., 2019, Wasik et al., 2018). In brief, a primer system was used that allows

433 polarity- and gene-specific detection of individual IAV vRNAs (Kawakami et al.,
434 2011). To enable absolute quantification, RNA reference standards were synthesized
435 and levels of vRNAs were calculated based on standard curves, as described
436 previously (Kupke et al., 2019).

437 For RT, 1 µL of the total RNA sample was combined with 1 µL of dNTPs (10 mM) and
438 1 µL of the RT primer (1 µM) and filled up to a volume of 15 µL with nuclease-free
439 water. Incubation was performed at 65°C for 5 min and 55°C for 5 min. During the
440 latter step, a pre-warmed mixture (55°C) consisting of 4 µL of 5x RT buffer, 0.5 µL
441 (100 U) Maxima H Minus reverse transcriptase, and 0.5 µL RiboLock RNase Inhibitor
442 (all reagents from Thermo Scientific) was added. RT primer: OP7, 5'-
443 ATTTAGGTGACACTATAGAAGCGACTGTGACTGCTGAAGTGGTG-3'; DI244, 5'-
444 ATTTAGGTGACACTATAGAAGCGAGCGAAAGCAGGTCAATTATATTC-3'. RT was
445 conducted for 30 min at 60°C, followed by 85°C for 5 min. Further, RNA reference
446 standards in 10-fold dilution steps were reverse transcribed. Next, the cDNA reaction
447 products were diluted to 100 µL in nuclease-free water. For qPCR, the Rotor-Gene Q
448 real-time PCR cycler (Qiagen) was used. The qPCR mix (10 µL) contained 1× Rotor-
449 Gene SYBR green PCR mix (Qiagen), 500 nM each primer, and 4 µL of diluted cDNA.
450 qPCR Primers: OP7, 5'-ATTTAGGTGACACTATAGAAGCG-3' and 5'-
451 CATTTGCCTAGCCCGAATC-3'; DI244, 5'- ATTTAGGTGACACTATAGAAGCG-3' and 5'-
452 GGAATCCCCTCAGTCTTC-3'. The PCR cycling conditions comprised: initial
453 denaturation step at 95°C for 5 min, followed by 40 PCR cycles of 95°C for 10 s and
454 62°C for 20 s.

Acknowledgement

We thank Nancy Wynserski for excellent technical assistance. This research was supported by a grant from the German Federal Ministry of Science and Education (Grant No. 01KI20140A). P.M.G. kindly acknowledges joint funding from the German Federal Ministry for Economic Affairs and Energy (BMWi), the European Social Fund (ESF), and the Max Planck Society (MPG) within the *EXIST Forschungstranfer* program (project 03EFMST030).

Author Contributions

Conceptualization, U.R. (Ulfert Rand), S.Y.K., L.C.S., U.R. (Udo Reichl) and D.B.; Investigation, U.R. (Ulfert Rand), H.S., M.D.H., T.H. and P.M.G.; Formal Analysis, U.R. (Ulfert Rand); Validation, U.R. (Ulfert Rand), H.S. and T.H.; Writing – Original Draft, S.Y.K.; Writing – Review & Editing, U.R. (Ulfert Rand), H.S., M.D.H., P.M.G., U.R. (Udo Reichl) and D.B.; Visualization, U.R. (Ulfert Rand) and S.Y.K.; Supervision, U.R. (Ulfert Rand), S.Y.K., L.C.S, U.R. (Udo Reichl) and D.B.; Project Administration, U.R. (Ulfert Rand), S.Y.K. and D.B.; Funding Acquisition, P.M.G., U.R. (Udo Reichl) and L.C.S.

Declaration of interests

A patent for the use of OP7 as an antiviral agent for treatment of IAV infection is pending. Patent holders are S.Y.K. and U.R. (Udo Reichl).

476 Another patent for the use of DI244 and OP7 as an antiviral agent for treatment of
477 coronavirus infection is pending. Patent holders are S.Y.K., U.R. (Udo Reichl), M.H.,
478 U.R. (Ulfert Rand), and D.B.

479 P.M.G. and U.R. (Udo Reichl) are inventors in a pending patent application detailing
480 the technology used for the chromatographic purification of the influenza virus
481 particles used in this study.

482

483 **Data availability**

484 Full dataset (of Fig. 1-4) is available in supplemental Table S1.

References

ABRAHAM, J. 2020. Passive antibody therapy in COVID-19. *Nat Rev Immunol,* 20**,** 401-403.

ALNAJI, F. G. & BROOKE, C. B. 2020. Influenza virus DI particles: Defective interfering or delightfully interesting? *PLoS Pathog,* 16**,** e1008436.

ANDREU-MORENO, I. & SANJUAN, R. 2020. Collective Viral Spread Mediated by Virion Aggregates Promotes the Evolution of Defective Interfering Particles. *Mbio,* 11.

BAUM, A., FULTON, B. O., WLOGA, E., COPIN, R., PASCAL, K. E., RUSSO, V., GIORDANO, S., LANZA, K., NEGRON, N., NI, M., WEI, Y., ATWAL, G. S., MURPHY, A. J., STAHL, N., YANCOPOULOS, G. D. & KYRATSOUS, C. A. 2020. Antibody cocktail to SARS-CoV-2 spike protein prevents rapid mutational escape seen with individual antibodies. *Science,* 369**,** 1014-1018.

BAUM, A. & GARCIA-SASTRE, A. 2011. Differential recognition of viral RNA by RIG-I. *Virulence,* 2**,** 166-9.

BEIGEL, J. H., TOMASHEK, K. M., DODD, L. E., MEHTA, A. K., ZINGMAN, B. S., KALIL, A. C., HOHMANN, E., CHU, H. Y., LUETKEMEYER, A., KLINE, S., LOPEZ DE CASTILLA, D., FINBERG, R. W., DIERBERG, K., TAPSON, V., HSIEH, L., PATTERSON, T. F., PAREDES, R., SWEENEY, D. A., SHORT, W. R., TOULOUMI, G., LYE, D. C., OHMAGARI, N., OH, M. D., RUIZ-PALACIOS, G. M., BENFIELD, T., FATKENHEUER, G., KORTEPETER, M. G., ATMAR, R. L., CREECH, C. B., LUNDGREN, J., BABIKER, A. G., PETT, S., NEATON, J. D., BURGESS, T. H., BONNETT, T., GREEN, M., MAKOWSKI, M., OSINUSI, A., NAYAK, S., LANE, H. C. & MEMBERS, A.-S. G. 2020. Remdesivir for the Treatment of Covid-19 - Final Report. *N Engl J Med,* 383**,** 1813-1826.

BOUDEWIJNS, R., THIBAUT, H. J., KAPTEIN, S. J. F., LI, R., VERGOTE, V., SELDESLACHTS, L., VAN WEYENBERGH, J., DE KEYZER, C., BERVOETS, L., SHARMA, S., LIESENBORGHS, L., MA, J., JANSEN, S., VAN LOOVEREN, D., VERCRUYSSE, T., WANG, X., JOCHMANS, D., MARTENS, E., ROOSE, K., DE VLIEGER, D., SCHEPENS, B., VAN BUYTEN, T., JACOBS, S., LIU, Y., MARTI-CARRERAS, J., VANMECHELEN, B., WAWINA-BOKALANGA, T., DELANG, L., ROCHA-PEREIRA, J., COELMONT, L., CHIU, W., LEYSSEN, P., HEYLEN, E., SCHOLS, D., WANG, L., CLOSE, L., MATTHIJNSSENS, J., VAN RANST, M., COMPERNOLLE, V., SCHRAMM, G., VAN LAERE, K., SAELENS, X., CALLEWAERT, N., OPDENAKKER, G., MAES, P., WEYNAND, B., CAWTHORNE, C., VANDE VELDE, G., WANG, Z., NEYTS, J. & DALLMEIER, K. 2020. STAT2 signaling restricts viral dissemination but drives severe pneumonia in SARS-CoV-2 infected hamsters. *Nat Commun,* 11**,** 5838.

BOULWARE, D. R., PULLEN, M. F., BANGDIWALA, A. S., PASTICK, K. A., LOFGREN, S. M., OKAFOR, E. C., SKIPPER, C. P., NASCENE, A. A., NICOL, M. R., ABASSI, M., ENGEN, N. W., CHENG, M. P., LABAR, D., LOTHER, S. A., MACKENZIE, L. J., DROBOT, G., MARTEN, N., ZARYCHANSKI, R., KELLY, L. E., SCHWARTZ, I. S., MCDONALD, E. G., RAJASINGHAM, R., LEE, T. C. & HULLSIEK, K. H. 2020. A Randomized Trial of Hydroxychloroquine as Postexposure Prophylaxis for Covid-19. *N Engl J Med,* 383**,** 517-525.

BROGGI, A., GHOSH, S., SPOSITO, B., SPREAFICO, R., BALZARINI, F., LO CASCIO, A., CLEMENTI, N., DE SANTIS, M., MANCINI, N., GRANUCCI, F. & ZANONI, I. 2020. Type III interferons disrupt the lung epithelial barrier upon viral recognition. *Science,* 369**,** 706-712.

BUSNADIEGO, I., FERNBACH, S., POHL, M. O., KARAKUS, U., HUBER, M., TRKOLA, A., STERTZ, S. & HALE, B. G. 2020. Antiviral Activity of Type I, II, and III Interferons Counterbalances ACE2 Inducibility and Restricts SARS-CoV-2. *mBio,* 11.

CAO, B., WANG, Y., WEN, D., LIU, W., WANG, J., FAN, G., RUAN, L., SONG, B., CAI, Y., WEI, M., LI, X., XIA, J., CHEN, N., XIANG, J., YU, T., BAI, T., XIE, X., ZHANG, L., LI, C., YUAN, Y., CHEN, H., LI, H., HUANG, H., TU, S., GONG, F., LIU, Y., WEI, Y., DONG, C., ZHOU, F., GU, X., XU, J., LIU, Z., ZHANG, Y., LI, H., SHANG, L., WANG, K., LI, K., ZHOU, X., DONG, X., QU, Z., LU, S., HU, X., RUAN, S., LUO, S., WU, J., PENG, L., CHENG, F., PAN, L., ZOU, J., JIA, C., WANG, J., LIU, X., WANG, S., WU, X., GE, Q., HE, J., ZHAN, H., QIU, F., GUO, L., HUANG, C., JAKI, T., HAYDEN, F.

534 G., HORBY, P. W., ZHANG, D. & WANG, C. 2020. A Trial of Lopinavir-Ritonavir in Adults
535 Hospitalized with Severe Covid-19. *N Engl J Med,* 382**,** 1787-1799.
536 CHAN, J. F., ZHANG, A. J., YUAN, S., POON, V. K., CHAN, C. C., LEE, A. C., CHAN, W. M., FAN, Z., TSOI,
537 H. W., WEN, L., LIANG, R., CAO, J., CHEN, Y., TANG, K., LUO, C., CAI, J. P., KOK, K. H., CHU, H.,
538 CHAN, K. H., SRIDHAR, S., CHEN, Z., CHEN, H., TO, K. K. & YUEN, K. Y. 2020. Simulation of the
539 Clinical and Pathological Manifestations of Coronavirus Disease 2019 (COVID-19) in a Golden
540 Syrian Hamster Model: Implications for Disease Pathogenesis and Transmissibility. *Clin Infect*
541 *Dis,* 71**,** 2428-2446.
542 CHEN, D. Y., KHAN, N., CLOSE, B. J., GOEL, R. K., BLUM, B., TAVARES, A. H., KENNEY, D., CONWAY, H.
543 L., EWOLDT, J. K., KAPELL, S., CHITALIA, V. C., CROSSLAND, N. A., CHEN, C. S., KOTTON, D. N.,
544 BAKER, S. C., CONNOR, J. H., DOUAM, F., EMILI, A. & SAEED, M. 2020a. SARS-CoV-2
545 desensitizes host cells to interferon through inhibition of the JAK-STAT pathway. *bioRxiv*.
546 CHEN, P., NIRULA, A., HELLER, B., GOTTLIEB, R. L., BOSCIA, J., MORRIS, J., HUHN, G., CARDONA, J.,
547 MOCHERLA, B., STOSOR, V., SHAWA, I., ADAMS, A. C., VAN NAARDEN, J., CUSTER, K. L., SHEN,
548 L., DURANTE, M., OAKLEY, G., SCHADE, A. E., SABO, J., PATEL, D. R., KLEKOTKA, P.,
549 SKOVRONSKY, D. M. & INVESTIGATORS, B.-. 2020b. SARS-CoV-2 Neutralizing Antibody LY-
550 CoV555 in Outpatients with Covid-19. *N Engl J Med*.
551 DIMMOCK, N. J., DOVE, B. K., SCOTT, P. D., MENG, B., TAYLOR, I., CHEUNG, L., HALLIS, B., MARRIOTT,
552 A. C., CARROLL, M. W. & EASTON, A. J. 2012. Cloned defective interfering influenza virus
553 protects ferrets from pandemic 2009 influenza A virus and allows protective immunity to be
554 established. *PLoS One,* 7**,** e49394.
555 DIMMOCK, N. J. & EASTON, A. J. 2014. Defective interfering influenza virus RNAs: time to reevaluate
556 their clinical potential as broad-spectrum antivirals? *J Virol,* 88**,** 5217-27.
557 DIMMOCK, N. J. & EASTON, A. J. 2015. Cloned Defective Interfering Influenza RNA and a Possible Pan-
558 Specific Treatment of Respiratory Virus Diseases. *Viruses,* 7**,** 3768-88.
559 DIMMOCK, N. J., RAINSFORD, E. W., SCOTT, P. D. & MARRIOTT, A. C. 2008. Influenza virus protecting
560 RNA: an effective prophylactic and therapeutic antiviral. *J Virol,* 82**,** 8570-8.
561 DOLGIN, E. 2021. Stocking the shelves for the next pandemic. *Nature,* 592**,** 340-343.
562 EASTON, A. J., SCOTT, P. D., EDWORTHY, N. L., MENG, B., MARRIOTT, A. C. & DIMMOCK, N. J. 2011. A
563 novel broad-spectrum treatment for respiratory virus infections: influenza-based defective
564 interfering virus provides protection against pneumovirus infection in vivo. *Vaccine,* 29**,**
565 2777-84.
566 FELGENHAUER, U., SCHOEN, A., GAD, H. H., HARTMANN, R., SCHAUBMAR, A. R., FAILING, K.,
567 DROSTEN, C. & WEBER, F. 2020. Inhibition of SARS-CoV-2 by type I and type III interferons. *J*
568 *Biol Chem,* 295**,** 13958-13964.
569 HARDING, A. T., HAAS, G. D., CHAMBERS, B. S. & HEATON, N. S. 2019. Influenza viruses that require
570 10 genomic segments as antiviral therapeutics. *Plos Pathogens,* 15.
571 HEIN, M. D., ARORA, P., MARICHAL-GALLARDO, P., WINKLER, M., GENZEL, Y., POHLMANN, S.,
572 SCHUGHART, K., KUPKE, S. Y. & REICHL, U. 2021a. Cell culture-based production and in vivo
573 characterization of purely clonal defective interfering influenza virus particles. *BMC Biol,* 19**,**
574 91.
575 HEIN, M. D., CHAWLA, A., CATTANEO, M., KUPKE, S. Y., GENZEL, Y. & REICHL, U. 2021b. Cell culture-
576 based production of defective interfering influenza A virus particles in perfusion mode using
577 an alternating tangential flow filtration system. *bioRxiv***,** 2021.06.07.446880.
578 HEIN, M. D., KOLLMUS, H., MARICHAL-GALLARDO, P., PUTTKER, S., BENNDORF, D., GENZEL, Y.,
579 SCHUGHART, K., KUPKE, S. Y. & REICHL, U. 2021c. OP7, a novel influenza A virus defective
580 interfering particle: production, purification, and animal experiments demonstrating antiviral
581 potential. *Appl Microbiol Biotechnol,* 105**,** 129-146.
582 HOAGLAND, D. A., MOLLER, R., UHL, S. A., OISHI, K., FRERE, J., GOLYNKER, I., HORIUCHI, S., PANIS, M.,
583 BLANCO-MELO, D., SACHS, D., ARKUN, K., LIM, J. K. & TENOEVER, B. R. 2021. Leveraging the
584 antiviral type I interferon system as a first line of defense against SARS-CoV-2 pathogenicity.
585 *Immunity*.

586 HOFFMANN, M., KLEINE-WEBER, H., SCHROEDER, S., KRUGER, N., HERRLER, T., ERICHSEN, S.,
587 SCHIERGENS, T. S., HERRLER, G., WU, N. H., NITSCHE, A., MULLER, M. A., DROSTEN, C. &
588 POHLMANN, S. 2020. SARS-CoV-2 Cell Entry Depends on ACE2 and TMPRSS2 and Is Blocked
589 by a Clinically Proven Protease Inhibitor. *Cell,* 181**,** 271-280 e8.
590 HORBY, P., LIM, W. S., EMBERSON, J. R., MAFHAM, M., BELL, J. L., LINSELL, L., STAPLIN, N.,
591 BRIGHTLING, C., USTIANOWSKI, A., ELMAHI, E., PRUDON, B., GREEN, C., FELTON, T.,
592 CHADWICK, D., REGE, K., FEGAN, C., CHAPPELL, L. C., FAUST, S. N., JAKI, T., JEFFERY, K.,
593 MONTGOMERY, A., ROWAN, K., JUSZCZAK, E., BAILLIE, J. K., HAYNES, R. & LANDRAY, M. J.
594 2020. Dexamethasone in Hospitalized Patients with Covid-19 - Preliminary Report. *N Engl J*
595 *Med*.
596 HUO, C., CHENG, J., XIAO, J., CHEN, M., ZOU, S., TIAN, H., WANG, M., SUN, L., HAO, Z. & HU, Y. 2020a.
597 Defective Viral Particles Produced in Mast Cells Can Effectively Fight Against Lethal Influenza
598 A Virus. *Front Microbiol,* 11**,** 553274.
599 HUO, C., TIAN, J., CHENG, J., XIAO, J., CHEN, M., ZOU, S., TIAN, H., WANG, M., SUN, H. & HU, Y.
600 2020b. Safety, Immunogenicity, and Effectiveness of Defective Viral Particles Arising in Mast
601 Cells Against Influenza in Mice. *Front Immunol,* 11**,** 585254.
602 JACKSON, L. A., ANDERSON, E. J., ROUPHAEL, N. G., ROBERTS, P. C., MAKHENE, M., COLER, R. N.,
603 MCCULLOUGH, M. P., CHAPPELL, J. D., DENISON, M. R., STEVENS, L. J., PRUIJSSERS, A. J.,
604 MCDERMOTT, A., FLACH, B., DORIA-ROSE, N. A., CORBETT, K. S., MORABITO, K. M., O'DELL,
605 S., SCHMIDT, S. D., SWANSON, P. A., 2ND, PADILLA, M., MASCOLA, J. R., NEUZIL, K. M.,
606 BENNETT, H., SUN, W., PETERS, E., MAKOWSKI, M., ALBERT, J., CROSS, K., BUCHANAN, W.,
607 PIKAART-TAUTGES, R., LEDGERWOOD, J. E., GRAHAM, B. S., BEIGEL, J. H. & M, R. N. A. S. G.
608 2020. An mRNA Vaccine against SARS-CoV-2 - Preliminary Report. *N Engl J Med,* 383**,** 1920-
609 1931.
610 KALBFUSS, B., KNOCHLEIN, A., KROBER, T. & REICHL, U. 2008. Monitoring influenza virus content in
611 vaccine production: precise assays for the quantitation of hemagglutination and
612 neuraminidase activity. *Biologicals,* 36**,** 145-61.
613 KAPTEIN, S. J. F., JACOBS, S., LANGENDRIES, L., SELDESLACHTS, L., TER HORST, S., LIESENBORGHS, L.,
614 HENS, B., VERGOTE, V., HEYLEN, E., BARTHELEMY, K., MAAS, E., DE KEYZER, C., BERVOETS, L.,
615 RYMENANTS, J., VAN BUYTEN, T., ZHANG, X., ABDELNABI, R., PANG, J., WILLIAMS, R.,
616 THIBAUT, H. J., DALLMEIER, K., BOUDEWIJNS, R., WOUTERS, J., AUGUSTIJNS, P.,
617 VEROUGSTRAETE, N., CAWTHORNE, C., BREUER, J., SOLAS, C., WEYNAND, B., ANNAERT, P.,
618 SPRIET, I., VANDE VELDE, G., NEYTS, J., ROCHA-PEREIRA, J. & DELANG, L. 2020. Favipiravir at
619 high doses has potent antiviral activity in SARS-CoV-2-infected hamsters, whereas
620 hydroxychloroquine lacks activity. *Proc Natl Acad Sci U S A,* 117**,** 26955-26965.
621 KAWAKAMI, E., WATANABE, T., FUJII, K., GOTO, H., WATANABE, S., NODA, T. & KAWAOKA, Y. 2011.
622 Strand-specific real-time RT-PCR for distinguishing influenza vRNA, cRNA, and mRNA. *J Virol*
623 *Methods,* 173**,** 1-6.
624 KONNO, Y., KIMURA, I., URIU, K., FUKUSHI, M., IRIE, T., KOYANAGI, Y., SAUTER, D., GIFFORD, R. J.,
625 CONSORTIUM, U.-C., NAKAGAWA, S. & SATO, K. 2020. SARS-CoV-2 ORF3b Is a Potent
626 Interferon Antagonist Whose Activity Is Increased by a Naturally Occurring Elongation
627 Variant. *Cell Rep,* 32**,** 108185.
628 KRAMMER, F. 2020. SARS-CoV-2 vaccines in development. *Nature,* 586**,** 516-527.
629 KUPKE, S. Y., LY, L. H., BORNO, S. T., RUFF, A., TIMMERMANN, B., VINGRON, M., HAAS, S. & REICHL,
630 U. 2020. Single-Cell Analysis Uncovers a Vast Diversity in Intracellular Viral Defective
631 Interfering RNA Content Affecting the Large Cell-to-Cell Heterogeneity in Influenza A Virus
632 Replication. *Viruses,* 12.
633 KUPKE, S. Y., RIEDEL, D., FRENSING, T., ZMORA, P. & REICHL, U. 2019. A Novel Type of Influenza A
634 Virus-Derived Defective Interfering Particle with Nucleotide Substitutions in Its Genome. *J*
635 *Virol,* 93.
636 LEE, J. S. & SHIN, E. C. 2020. The type I interferon response in COVID-19: implications for treatment.
637 *Nat Rev Immunol,* 20**,** 585-586.

638 LEI, X., DONG, X., MA, R., WANG, W., XIAO, X., TIAN, Z., WANG, C., WANG, Y., LI, L., REN, L., GUO, F.,
639 ZHAO, Z., ZHOU, Z., XIANG, Z. & WANG, J. 2020. Activation and evasion of type I interferon
640 responses by SARS-CoV-2. *Nat Commun,* 11**,** 3810.
641 LOGUNOV, D. Y., DOLZHIKOVA, I. V., ZUBKOVA, O. V., TUKHVATULLIN, A. I., SHCHEBLYAKOV, D. V.,
642 DZHARULLAEVA, A. S., GROUSOVA, D. M., EROKHOVA, A. S., KOVYRSHINA, A. V., BOTIKOV, A.
643 G., IZHAEVA, F. M., POPOVA, O., OZHAROVSKAYA, T. A., ESMAGAMBETOV, I. B.,
644 FAVORSKAYA, I. A., ZRELKIN, D. I., VORONINA, D. V., SHCHERBININ, D. N., SEMIKHIN, A. S.,
645 SIMAKOVA, Y. V., TOKARSKAYA, E. A., LUBENETS, N. L., EGOROVA, D. A., SHMAROV, M. M.,
646 NIKITENKO, N. A., MOROZOVA, L. F., SMOLYARCHUK, E. A., KRYUKOV, E. V., BABIRA, V. F.,
647 BORISEVICH, S. V., NARODITSKY, B. S. & GINTSBURG, A. L. 2020. Safety and immunogenicity
648 of an rAd26 and rAd5 vector-based heterologous prime-boost COVID-19 vaccine in two
649 formulations: two open, non-randomised phase 1/2 studies from Russia. *Lancet,* 396**,** 887-
650 897.
651 MARICHAL-GALLARDO, P., BORNER, K., PIELER, M. M., SONNTAG-BUCK, V., OBR, M., BEJARANO, D.,
652 WOLFF, M. W., KRAUSSLICH, H. G., REICHL, U. & GRIMM, D. 2021. Single-Use Capture
653 Purification of Adeno-Associated Viral Gene Transfer Vectors by Membrane-Based Steric
654 Exclusion Chromatography. *Hum Gene Ther*.
655 MARICHAL-GALLARDO, P., PIELER, M. M., WOLFF, M. W. & REICHL, U. 2017. Steric exclusion
656 chromatography for purification of cell culture-derived influenza A virus using regenerated
657 cellulose membranes and polyethylene glycol. *J Chromatogr A,* 1483**,** 110-119.
658 MEIR, M., HAREL, N., MILLER, D., GELBART, M., ELDAR, A., GOPHNA, U. & STERN, A. 2020.
659 Competition between social cheater viruses is driven by mechanistically different cheating
660 strategies. *Science Advances,* 6.
661 MONK, P. D., MARSDEN, R. J., TEAR, V. J., BROOKES, J., BATTEN, T. N., MANKOWSKI, M., GABBAY, F.
662 J., DAVIES, D. E., HOLGATE, S. T., HO, L. P., CLARK, T., DJUKANOVIC, R., WILKINSON, T. M. A. &
663 INHALED INTERFERON BETA, C.-S. G. 2020. Safety and efficacy of inhaled nebulised
664 interferon beta-1a (SNG001) for treatment of SARS-CoV-2 infection: a randomised, double-
665 blind, placebo-controlled, phase 2 trial. *Lancet Respir Med*.
666 PALACIOS, R., PATINO, E. G., DE OLIVEIRA PIORELLI, R., CONDE, M., BATISTA, A. P., ZENG, G., XIN, Q.,
667 KALLAS, E. G., FLORES, J., OCKENHOUSE, C. F. & GAST, C. 2020. Double-Blind, Randomized,
668 Placebo-Controlled Phase III Clinical Trial to Evaluate the Efficacy and Safety of treating
669 Healthcare Professionals with the Adsorbed COVID-19 (Inactivated) Vaccine Manufactured by
670 Sinovac - PROFISCOV: A structured summary of a study protocol for a randomised controlled
671 trial. *Trials,* 21**,** 853.
672 PAN, H., PETO, R., HENAO-RESTREPO, A. M., PREZIOSI, M. P., SATHIYAMOORTHY, V., ABDOOL KARIM,
673 Q., ALEJANDRIA, M. M., HERNANDEZ GARCIA, C., KIENY, M. P., MALEKZADEH, R., MURTHY, S.,
674 REDDY, K. S., ROSES PERIAGO, M., ABI HANNA, P., ADER, F., AL-BADER, A. M., ALHASAWI, A.,
675 ALLUM, E., ALOTAIBI, A., ALVAREZ-MORENO, C. A., APPADOO, S., ASIRI, A., AUKRUST, P.,
676 BARRATT-DUE, A., BELLANI, S., BRANCA, M., CAPPEL-PORTER, H. B. C., CERRATO, N., CHOW,
677 T. S., COMO, N., EUSTACE, J., GARCIA, P. J., GODBOLE, S., GOTUZZO, E., GRISKEVICIUS, L.,
678 HAMRA, R., HASSAN, M., HASSANY, M., HUTTON, D., IRMANSYAH, I., JANCORIENE, L.,
679 KIRWAN, J., KUMAR, S., LENNON, P., LOPARDO, G., LYDON, P., MAGRINI, N., MAGUIRE, T.,
680 MANEVSKA, S., MANUEL, O., MCGINTY, S., MEDINA, M. T., MESA RUBIO, M. L., MIRANDA-
681 MONTOYA, M. C., NEL, J., NUNES, E. P., PEROLA, M., PORTOLES, A., RASMIN, M. R., RAZA, A.,
682 REES, H., REGES, P. P. S., ROGERS, C. A., SALAMI, K., SALVADORI, M. I., SINANI, N., STERNE, J.
683 A. C., STEVANOVIKJ, M., TACCONELLI, E., TIKKINEN, K. A. O., TRELLE, S., ZAID, H., ROTTINGEN,
684 J. A. & SWAMINATHAN, S. 2020. Repurposed Antiviral Drugs for Covid-19 - Interim WHO
685 Solidarity Trial Results. *N Engl J Med*.
686 REHWINKEL, J., TAN, C. P., GOUBAU, D., SCHULZ, O., PICHLMAIR, A., BIER, K., ROBB, N., VREEDE, F.,
687 BARCLAY, W., FODOR, E. & REIS E SOUSA, C. 2010. RIG-I detects viral genomic RNA during
688 negative-strand RNA virus infection. *Cell,* 140**,** 397-408.

SCOTT, P. D., MENG, B., MARRIOTT, A. C., EASTON, A. J. & DIMMOCK, N. J. 2011. Defective interfering influenza A virus protects in vivo against disease caused by a heterologous influenza B virus. *J Gen Virol,* 92**,** 2122-2132.

SLEIJFER, S., BANNINK, M., VAN GOOL, A. R., KRUIT, W. H. & STOTER, G. 2005. Side effects of interferon-alpha therapy. *Pharm World Sci,* 27**,** 423-31.

STERNE, J. A. C., MURTHY, S., DIAZ, J. V., SLUTSKY, A. S., VILLAR, J., ANGUS, D. C., ANNANE, D., AZEVEDO, L. C. P., BERWANGER, O., CAVALCANTI, A. B., DEQUIN, P. F., DU, B., EMBERSON, J., FISHER, D., GIRAUDEAU, B., GORDON, A. C., GRANHOLM, A., GREEN, C., HAYNES, R., HEMING, N., HIGGINS, J. P. T., HORBY, P., JUNI, P., LANDRAY, M. J., LE GOUGE, A., LECLERC, M., LIM, W. S., MACHADO, F. R., MCARTHUR, C., MEZIANI, F., MOLLER, M. H., PERNER, A., PETERSEN, M. W., SAVOVIC, J., TOMAZINI, B., VEIGA, V. C., WEBB, S. & MARSHALL, J. C. 2020. Association Between Administration of Systemic Corticosteroids and Mortality Among Critically Ill Patients With COVID-19: A Meta-analysis. *JAMA,* 324**,** 1330-1341.

TANNER, E. J., KIRKEGAARD, K. A. & WEINBERGER, L. S. 2016. Exploiting Genetic Interference for Antiviral Therapy. *PLoS Genet,* 12**,** e1005986.

TAPIA, F., LASKE, T., WASIK, M. A., RAMMHOLD, M., GENZEL, Y. & REICHL, U. 2019. Production of Defective Interfering Particles of Influenza A Virus in Parallel Continuous Cultures at Two Residence Times-Insights From qPCR Measurements and Viral Dynamics Modeling. *Frontiers in Bioengineering and Biotechnology,* 7.

TOMAZINI, B. M., MAIA, I. S., CAVALCANTI, A. B., BERWANGER, O., ROSA, R. G., VEIGA, V. C., AVEZUM, A., LOPES, R. D., BUENO, F. R., SILVA, M., BALDASSARE, F. P., COSTA, E. L. V., MOURA, R. A. B., HONORATO, M. O., COSTA, A. N., DAMIANI, L. P., LISBOA, T., KAWANO-DOURADO, L., ZAMPIERI, F. G., OLIVATO, G. B., RIGHY, C., AMENDOLA, C. P., ROEPKE, R. M. L., FREITAS, D. H. M., FORTE, D. N., FREITAS, F. G. R., FERNANDES, C. C. F., MELRO, L. M. G., JUNIOR, G. F. S., MORAIS, D. C., ZUNG, S., MACHADO, F. R., AZEVEDO, L. C. P. & INVESTIGATORS, C. C.-B. I. 2020. Effect of Dexamethasone on Days Alive and Ventilator-Free in Patients With Moderate or Severe Acute Respiratory Distress Syndrome and COVID-19: The CoDEX Randomized Clinical Trial. *JAMA,* 324**,** 1307-1316.

VIGNUZZI, M. & LOPEZ, C. B. 2019. Defective viral genomes are key drivers of the virus-host interaction. *Nat Microbiol,* 4**,** 1075-1087.

VOYSEY, M., CLEMENS, S. A. C., MADHI, S. A., WECKX, L. Y., FOLEGATTI, P. M., ALEY, P. K., ANGUS, B., BAILLIE, V. L., BARNABAS, S. L., BHORAT, Q. E., BIBI, S., BRINER, C., CICCONI, P., COLLINS, A. M., COLIN-JONES, R., CUTLAND, C. L., DARTON, T. C., DHEDA, K., DUNCAN, C. J. A., EMARY, K. R. W., EWER, K. J., FAIRLIE, L., FAUST, S. N., FENG, S., FERREIRA, D. M., FINN, A., GOODMAN, A. L., GREEN, C. M., GREEN, C. A., HEATH, P. T., HILL, C., HILL, H., HIRSCH, I., HODGSON, S. H. C., IZU, A., JACKSON, S., JENKIN, D., JOE, C. C. D., KERRIDGE, S., KOEN, A., KWATRA, G., LAZARUS, R., LAWRIE, A. M., LELLIOTT, A., LIBRI, V., LILLIE, P. J., MALLORY, R., MENDES, A. V. A., MILAN, E. P., MINASSIAN, A. M., MCGREGOR, A., MORRISON, H., MUJADIDI, Y. F., NANA, A., O'REILLY, P. J., PADAYACHEE, S. D., PITTELLA, A., PLESTED, E., POLLOCK, K. M., RAMASAMY, M. N., RHEAD, S., SCHWARZBOLD, A. V., SINGH, N., SMITH, A., SONG, R., SNAPE, M. D., SPRINZ, E., SUTHERLAND, R. K., TARRANT, R., THOMSON, E. C., TOROK, M. E., TOSHNER, M., TURNER, D. P. J., VEKEMANS, J., VILLAFANA, T. L., WATSON, M. E. E., WILLIAMS, C. J., DOUGLAS, A. D., HILL, A. V. S., LAMBE, T., GILBERT, S. C., POLLARD, A. J. & OXFORD, C. V. T. G. 2020. Safety and efficacy of the ChAdOx1 nCoV-19 vaccine (AZD1222) against SARS-CoV-2: an interim analysis of four randomised controlled trials in Brazil, South Africa, and the UK. *Lancet*.

WALSH, E. E., FRENCK, R. W., JR., FALSEY, A. R., KITCHIN, N., ABSALON, J., GURTMAN, A., LOCKHART, S., NEUZIL, K., MULLIGAN, M. J., BAILEY, R., SWANSON, K. A., LI, P., KOURY, K., KALINA, W., COOPER, D., FONTES-GARFIAS, C., SHI, P. Y., TURECI, O., TOMPKINS, K. R., LYKE, K. E., RAABE, V., DORMITZER, P. R., JANSEN, K. U., SAHIN, U. & GRUBER, W. C. 2020. Safety and Immunogenicity of Two RNA-Based Covid-19 Vaccine Candidates. *N Engl J Med*.

740 WANG, Y., ZHANG, D., DU, G., DU, R., ZHAO, J., JIN, Y., FU, S., GAO, L., CHENG, Z., LU, Q., HU, Y., LUO,
741 G., WANG, K., LU, Y., LI, H., WANG, S., RUAN, S., YANG, C., MEI, C., WANG, Y., DING, D., WU,
742 F., TANG, X., YE, X., YE, Y., LIU, B., YANG, J., YIN, W., WANG, A., FAN, G., ZHOU, F., LIU, Z., GU,
743 X., XU, J., SHANG, L., ZHANG, Y., CAO, L., GUO, T., WAN, Y., QIN, H., JIANG, Y., JAKI, T.,
744 HAYDEN, F. G., HORBY, P. W., CAO, B. & WANG, C. 2020. Remdesivir in adults with severe
745 COVID-19: a randomised, double-blind, placebo-controlled, multicentre trial. *Lancet,* 395**,**
746 1569-1578.
747 WASIK, M. A., EICHWALD, L., GENZEL, Y. & REICHL, U. 2018. Cell culture-based production of
748 defective interfering particles for influenza antiviral therapy. *Appl Microbiol Biotechnol,* 102**,**
749 1167-1177.
750 YANG, Y. C., LYU, T. B., ZHOU, R. N., HE, X. E., YE, K. Y., XIE, Q., ZHU, L., CHEN, T. T., SHEN, C., WU, Q.
751 H., ZHANG, B. & ZHAO, W. 2019. The Antiviral and Antitumor Effects of Defective Interfering
752 Particles/Genomes and Their Mechanisms. *Frontiers in Microbiology,* 10.
753 YINDA, C. K., PORT, J. R., BUSHMAKER, T., OFFEI OWUSU, I., PURUSHOTHAM, J. N., AVANZATO, V. A.,
754 FISCHER, R. J., SCHULZ, J. E., HOLBROOK, M. G., HEBNER, M. J., ROSENKE, R., THOMAS, T.,
755 MARZI, A., BEST, S. M., DE WIT, E., SHAIA, C., VAN DOREMALEN, N. & MUNSTER, V. J. 2021.
756 K18-hACE2 mice develop respiratory disease resembling severe COVID-19. *PLoS Pathog,* 17**,**
757 e1009195.
758 ZHANG, N. N., SHEN, S. H., JIANG, L. J., ZHANG, W., ZHANG, H. X., SUN, Y. P., LI, X. Y., HUANG, Q. H.,
759 GE, B. X., CHEN, S. J., WANG, Z. G., CHEN, Z. & ZHU, J. 2008. RIG-I plays a critical role in
760 negatively regulating granulocytic proliferation. *Proc Natl Acad Sci U S A,* 105**,** 10553-8.
761 ZHAO, H., TO, K. K. W., CHU, H., DING, Q., ZHAO, X., LI, C., SHUAI, H., YUAN, S., ZHOU, J., KOK, K. H.,
762 JIANG, S. & YUEN, K. Y. 2018. Dual-functional peptide with defective interfering genes
763 effectively protects mice against avian and seasonal influenza. *Nat Commun,* 9**,** 2358.
764 ZIEGLER, C. G. K., ALLON, S. J., NYQUIST, S. K., MBANO, I. M., MIAO, V. N., TZOUANAS, C. N., CAO, Y.,
765 YOUSIF, A. S., BALS, J., HAUSER, B. M., FELDMAN, J., MUUS, C., WADSWORTH, M. H., 2ND,
766 KAZER, S. W., HUGHES, T. K., DORAN, B., GATTER, G. J., VUKOVIC, M., TALIAFERRO, F., MEAD,
767 B. E., GUO, Z., WANG, J. P., GRAS, D., PLAISANT, M., ANSARI, M., ANGELIDIS, I., ADLER, H.,
768 SUCRE, J. M. S., TAYLOR, C. J., LIN, B., WAGHRAY, A., MITSIALIS, V., DWYER, D. F., BUCHHEIT,
769 K. M., BOYCE, J. A., BARRETT, N. A., LAIDLAW, T. M., CARROLL, S. L., COLONNA, L., TKACHEV,
770 V., PETERSON, C. W., YU, A., ZHENG, H. B., GIDEON, H. P., WINCHELL, C. G., LIN, P. L., BINGLE,
771 C. D., SNAPPER, S. B., KROPSKI, J. A., THEIS, F. J., SCHILLER, H. B., ZARAGOSI, L. E., BARBRY, P.,
772 LESLIE, A., KIEM, H. P., FLYNN, J. L., FORTUNE, S. M., BERGER, B., FINBERG, R. W., KEAN, L. S.,
773 GARBER, M., SCHMIDT, A. G., LINGWOOD, D., SHALEK, A. K., ORDOVAS-MONTANES, J., LUNG-
774 NETWORK@HUMANCELLATLAS.ORG, H. C. A. L. B. N. E. A. & NETWORK, H. C. A. L. B. 2020.
775 SARS-CoV-2 Receptor ACE2 Is an Interferon-Stimulated Gene in Human Airway Epithelial Cells
776 and Is Detected in Specific Cell Subsets across Tissues. *Cell,* 181**,** 1016-1035 e19.
777 ZIEGLER, C. M. & BOTTEN, J. W. 2020. Defective Interfering Particles of Negative-Strand RNA Viruses.
778 *Trends in Microbiology,* 28**,** 554-565.

779